Symposium 2016 of the South African Ballistic Organization
Cape Town, South Africa 27-29 September 2016

EVALUATION OF SACRIFICIAL MATERIALS AGAINST SPHERICAL FRAGMENTS IN A SEMI-CONFINED BLAST CHAMBER

Z Jiba[*], IM Snyman, L Shoke and TJ Sono

Landwards Sciences, Defence Peace Safety and Security
Council for Scientific and Industrial Research (CSIR)
Pretoria, South Africa

Email: zjiba@csir.co.za

The purpose of this work is to evaluate sacrificial materials that can be used in the blast chamber during the detonation of encased charges. This paper details the evaluation of sacrificial materials arranged in an arena manner and the damage observed on the backing steel plates located behind the sacrificial layers exposed to 2 mm Chromium steel balls in a semi-confined environment. Conveyor belt, Polyurea / 1.6 mm mild steel material, Shutter board and Supawood were evaluated as sacrificial materials and were found to provide some degree of protection against the fragments. After detonation on each test, all the sacrificial materials evaluated had some degree of structural integrity, blast and thermal resistance as they were able to withstand the heat from blast signature for the duration at which they were evaluated. The average spread of fragments on the buffer plate behind the materials was found to be between 325-420 mm which correlates with the prediction form the mathematical models. The Polyurea/1.6 mm steel composite and Shutter board performed best according to the evaluation.

Key words: Chromium Steel grade 40 fragments Pre-formed fragmented charge, sacrificial material, SEmily

1 INTRODUCTION

The CSIR has commissioned a 6 m length, 5 m diameter and 30 mm thick enclosed blast chamber Emily in 2010, which consists of a sectioned part of the decommissioned Daphne submarine, Emily Hob-house. The blast chamber has been used successfully to characterise several types of charges within an enclosed environment in collaboration with industry (Snyman et al. , 2013). Warheads deployed in theatre of operations can also be characterised within this blast chamber to quantify their blast and thermal signature. However, warheads can potentially accelerate fragments produced from their container materials with a potential to damage the wall of the chamber and thus degrading its lifespan. A sacrificial layer is therefore required to catch the fragments and stop them from damaging the inner wall of the blast chamber.

Tests were previously conducted to evaluate the potential materials that can be used as a sacrificial layer in a form of a liner within Emily (Shoke et al., 2014). Sacrificial layers tested were made of the following materials: Conveyor belt, Shutter board, Supawood, Polyurea layer on 1.6 mm mild steel plate and Polystone. During those tests, fragments with mass of 2.5 g, made from Al 6082 disc with an outer diameter (OD) of 20 mm and thickness of 3 mm, were accelerated at a speed of 2000 m/s and impacted the free standing target material positioned at a stand of distance (SOD) of 2 m. Amongst these materials, the Conveyor belt was found to perform better.

Subsequently, these sacrificial layers were furthermore evaluated but with a backing block behind to mimic the walls of Emily instead of free standing and were arranged in an Arena setup. Multiple fragments in a form of steel balls (OD =4.8 mm) were propelled at a velocity of 1800 m/s to impact the backed sacrificial material located at an SOD of 2 m.. During these tests, the conveyor belt material was found to be the weakest while shutter board Polyurea/steel composite were found to be the most protective (Shoke et al. , 2014). During the previous tests, the sacrificial materials were not exposed to enhanced blast as they were evaluated in free air. Some of these promising materials may not necessary be compatible enhanced blast and thermal signature resulting from the multiple reflections within the blast chamber.

To evaluate the sacrificial layers in a typical enhanced blast environment, a scaled Emily (SEmily) was used to further characterise the selected materials. SEmily is a 1.2 m long, 1 m diameter blast chamber. The curved and back wall of SEmily consists of 10 mm thick commercially graded mild steel (Snyman et al., 2016). Selected materials were layered onto a 3.2 mm mild steel layer, attached to the inner walls of SEmily and subsequently exposed to fragments from the pre-fragmented explosive charge. A 24 g cylindrical PE4 charge, containing 2 mm Chromium-steel grade 40 balls were used as a source of fragments.

2 CHARGE DESIGN- SPHERICAL STEEL FRAGMENTS

Figure 1 shows a layout of the charge assembly consisting of a PE4 cylindrical charge, steel balls and the canister material made of Polyethylene. The PE4 cylindrical charge with radius (r_C) was placed in direct contact with the balls with an effective thickness (t). Cylindrical Gurney equations were employed in this configuration to estimate the dimensions of the charge and balls required to achieve terminal velocity of 1700 m/s.

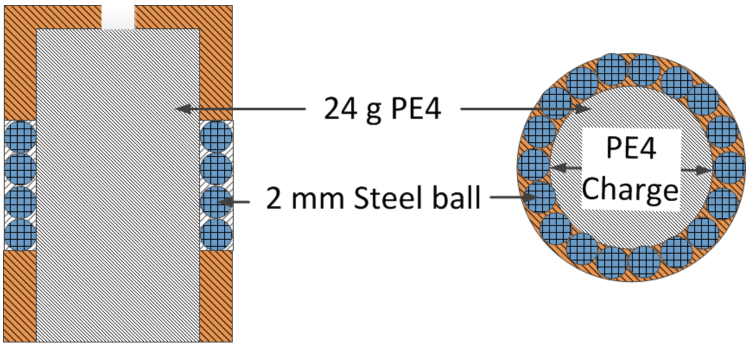

Figure 1: Explosive charge assembly.

The relationship between the terminal velocity of the fragment and the mass of the explosive per unit length is given by a cylindrical Gurney model as in Equation 1 (Kennedy , 1998)(Kennedy , 1998) .

$$\frac{v}{\sqrt{2E}} = \left(\frac{M}{C} + \frac{1}{2}\right)^{-\frac{1}{2}} \qquad 1$$

In Equation 1, M is the metal mass, C is the explosive charge mass and v is the velocity of one of the fragments. The desired terminal velocity of the fragment is 1700 m/s accelerated by a PE4 explosive charge that has a Gurney characteristic velocity $\sqrt{2E}$ = 2660 m/s. From Equation 2, knowing the velocity of detonation, D,

$$\sqrt{2E} = \frac{D}{2.97} \quad , \qquad 2$$

yielded $\frac{v}{\sqrt{2E}} = 0.64$. The metal-to-charge ratio, M/C of 1.73 was subsequently determined from Equation 1. The metal-to-charge mass ratio can further be written as:

$$\frac{M}{C} = \frac{\rho_m V_m}{\rho_c V_c} \qquad 3$$

where ρ_m, ρ_c are the densities and V_m, V_c are the volumes of the metal and charge, respectively. Spherical steel balls with an OD of 2 mm were used as fragments and arranged in a single layer inside a cylindrical mould, leading to the total thickness of the metal as 2 mm, as shown in Figure 2.

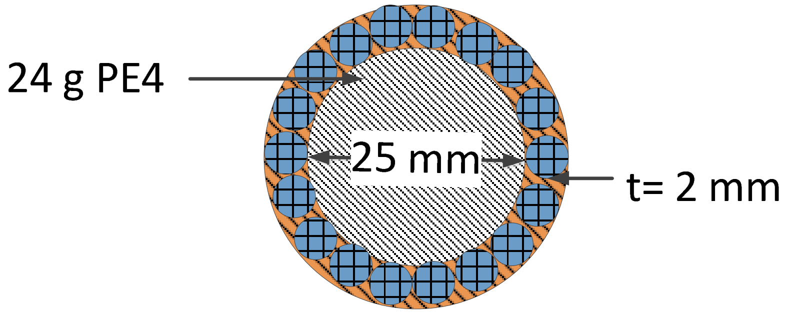

Figure 2: Layout of the metal and explosive charge.

Further manipulation of Equation 3 resulted with M/C being determined as in Equation 4. M/C, ρ_m, ρ_c and t were used to determine r_c required to propel the balls at the required velocity. Equation 5 shows all known parameters substituted in Equation 4, leaving only r_c unknown.

$$\frac{M}{C} = \frac{\rho_m}{\rho_c}\left(\frac{t^3 + 3t^2 r_c + 3t * r_c^2}{r_c^3}\right) \qquad 4$$

$$\frac{M}{C} = \frac{7.8}{1.55}\left(\frac{2^3 + 3 * 2^2 * 12.5 + 3 * 2 * r_c^2}{r_c^3}\right) = 1.73 \qquad 5$$

For a metal with thickness of 2 mm to be propelled at 1700 m/s, the radius of the explosive charge per unit area should be 12.5 mm as shown in Table 1.

Table 1: Summary of a Cylindrical Gurney model and charge dimensions

Parameter	$\sqrt{2E}$	M/C	ρ_m	t	ρ_c	r_c	D
Unit	m/s		g/cm^3	mm	g/cm^3	mm	m/s
Value	2525	1.73	7.8	2.0	1.55	12.5	7500

3 EXPERIMENTAL SETUP

3.1 Test Description

The testing of the sacrificial layers was executed at DBEL in T7 test range within SEmily. Figure 3 shows the general setup of SEmily. Polyurea/steel composite, Shutter board, Supawood and Conveyer belt material were located as shown on the front view of Figure 3. A 3.2 mm thick steel sleeve cylinder with a diameter of 0.99 m was used as a buffer between SEmily and the sacrificial materials. The sacrificial layers were placed on the inside walls of the steel sleeve and positioned in place through the use of a steel ring. The steel sleeve was sectioned in four parts and labelled A, B, C and D. Layer A was a shutter board material, B was Supawood, C was Conveyor belt material and D was Polyurea/1.6 mild steel. Two steel frame rings secured the sacrificial materials.

Two tests were executed with the same materials, while keeping track of the penetrations into the buffer plate.

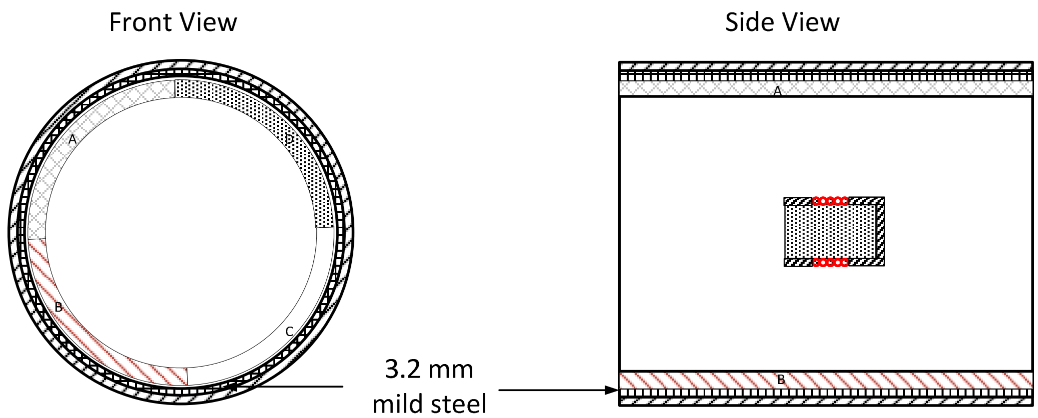

Figure 3: General setup for the evaluation of the sacrificial materials.

3.2 Charge Setup

The encased explosive charge was prepared as shown in Figure 4(a). A 24 g PE4 charge was moulded in an assembly consisting of polyethylene cup of 11 mm length, the bandwidth of steel balls is 10 mm (centre to centre). The number of balls per charge is 210 and therefore per quarter section is about 53. The mould had an inner diameter of 25 mm, 2 mm thickness and length of 31 mm. A 6.5 mm diameter hole was opened on the cup to house M2A2 detonator. The encased explosive charge was hanging from the top of SEmily as shown in Figure 4(b).

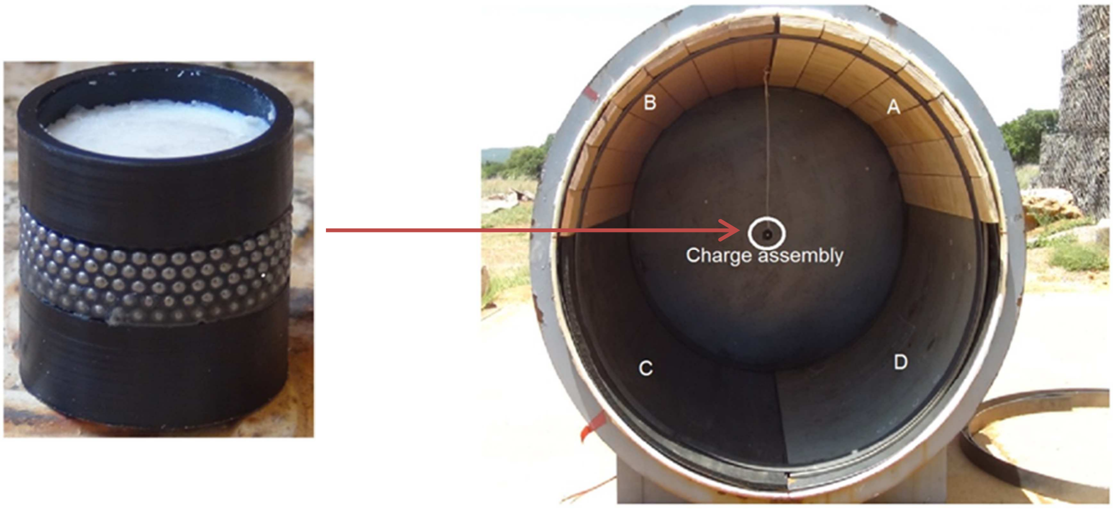

(a) close-up view of the explosive charge assembly

(b) Arrangement of the explosive charge in SEmily

Figure 4: The charge set-up inside SEmily

4 COMPUTATIONAL ANALYSIS

4.1 Computational Model

The objective of the computational analysis was to quantify the terminal spatial dynamics of the fragments based on the initial configuration of the charge assembly as depicted in Figure 4. Figure 5 shows a schematic layout and dimensions of the charge, balls, container and the detonator and Figure 6 shows the proposed test layout. Minimum spread of the ball bearings on arrival at the walls of the chamber is desired to ensure that they do not escape outside or damage the closed wall of SEmily.

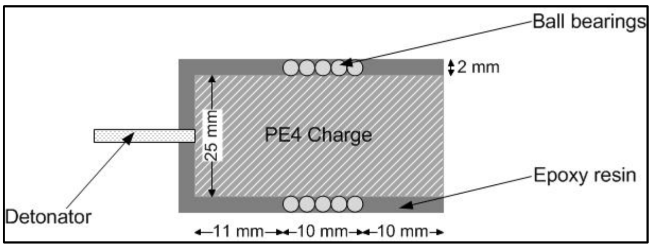

Figure 5: Schematic of pre-fragmented charge

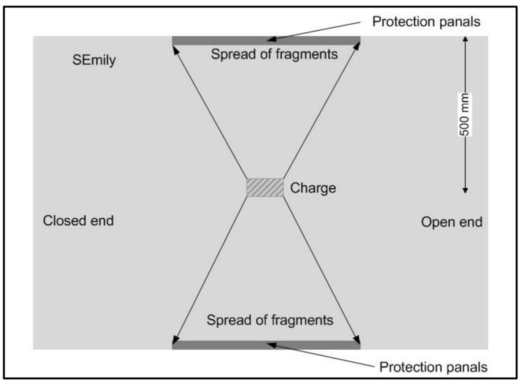

Figure 6: Schematic of proposed test set-up

Figure 7(a) shows the quarter symmetry three-dimensional model of the spheres located in a 10 mm bandwidth. Note that the balls are packed somewhat different from Figure 4(a). The detonation point is indicated. Increasing the number of spheres in the axial direction on the explosive charge estimates the spread of the number of fragments on the inner surface of SEmily. Figure 7(b) shows adding a row towards the closed and the open end of SEmily, in other words, one row closer to the detonator and one further away from the detonator.

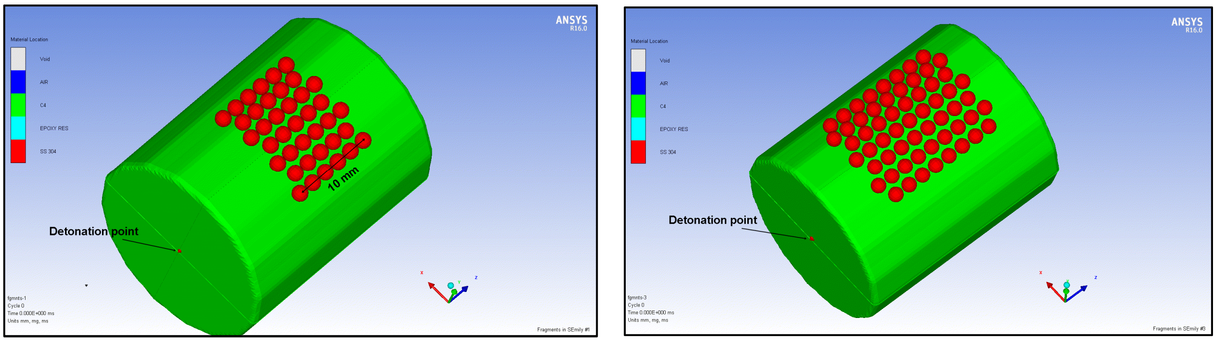

(a) Row of spheres along the surface of the charge (b) One sphere added on closed and open end

Figure 7: The three dimensional set-up, reflected about the symmetry planes

Table 2 gives the material models and parameter sets from the internal AUTODYN Material Library, based on published material data.

Table 2: Material models and parameters sets

Items	Material	Parameter set	Equation of state	Strength model
Atmosphere	Air	Air	Ideal	-
Charge	PE4	C4	JWL	-
Spherical fragments	Steel	AISI 1006	Shock	Johnson-Cook
Container	Epoxy	Epoxy Resin	Shock	-

4.2 Computational Results

The first results of the quarter symmetry computational model indicated that the balls might break due to the detonation that introduced a sudden acceleration over a very short time. Figure 8(a) shows the detonation and expansion of the gas by-products at six microseconds after detonation. The gas surrounds and obscures the relative position of the balls. The gas continues to expand while the balls are gathering speed. Figure 8(b) shows a snapshot at 13.5 microseconds with the gas escaping across the outside boundary of the Euler mesh. Some of the balls are highly deformed and are obscured by the surrounding gas. Note that the model was reflected about the xz-symmetry plane.

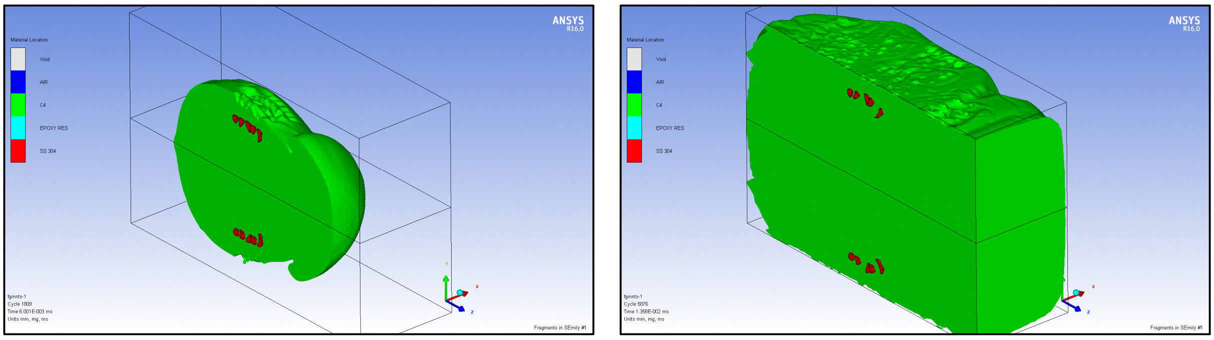

(a) Snapshot at 6 microseconds (b) Snapshot at 13.5 microseconds

Figure 8: Snapshots of detonation computation

Figure 9 shows the balls after 15.3 microseconds without the surrounding explosive gas. The computation of the material response of the balls is restricted to plastic deformation according to the Johnson-Cook model and cannot predict fracture. However, the shape of the balls indicates severe deformation that implies fracture Due to this excessive deformation, it may be assumed that some of these balls might fracture.

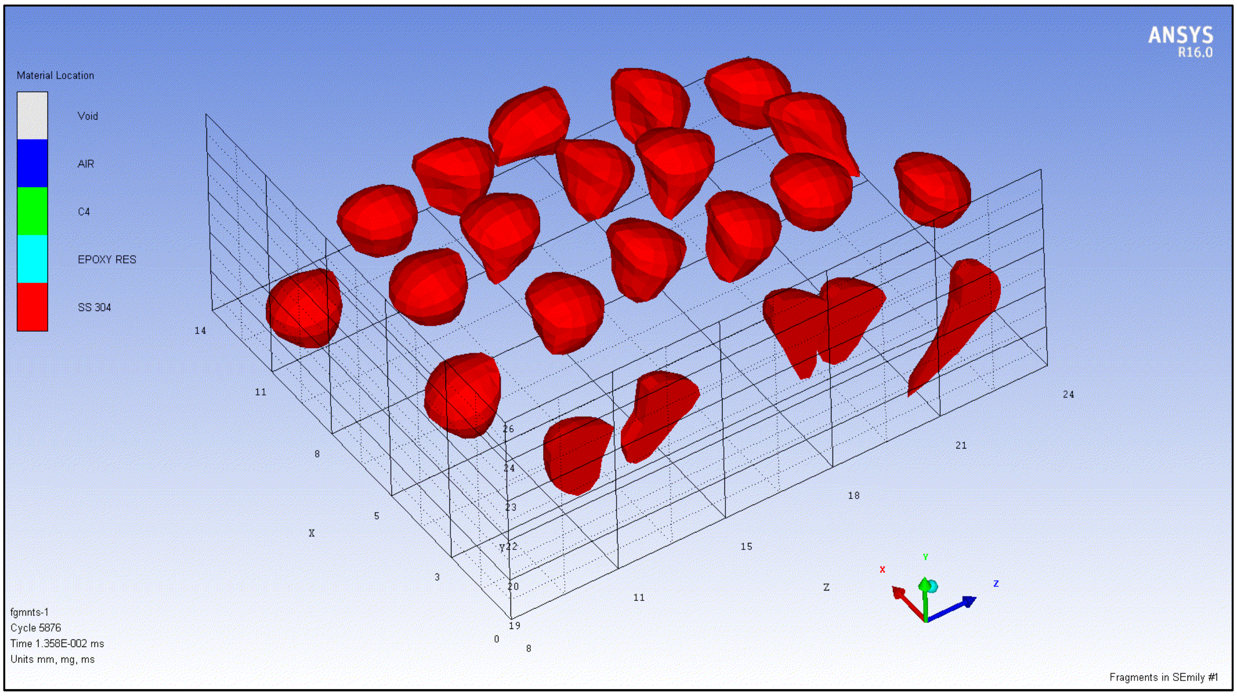

Figure 9: The position of the balls after 13.5 microseconds

Figure 10 shows the computed relative position of selected spheres on the inside surface (at 500 mm) of SEmily for the 10 mm bandwidth. The spread was calculated to be 198 mm. Detonation is from left to right.

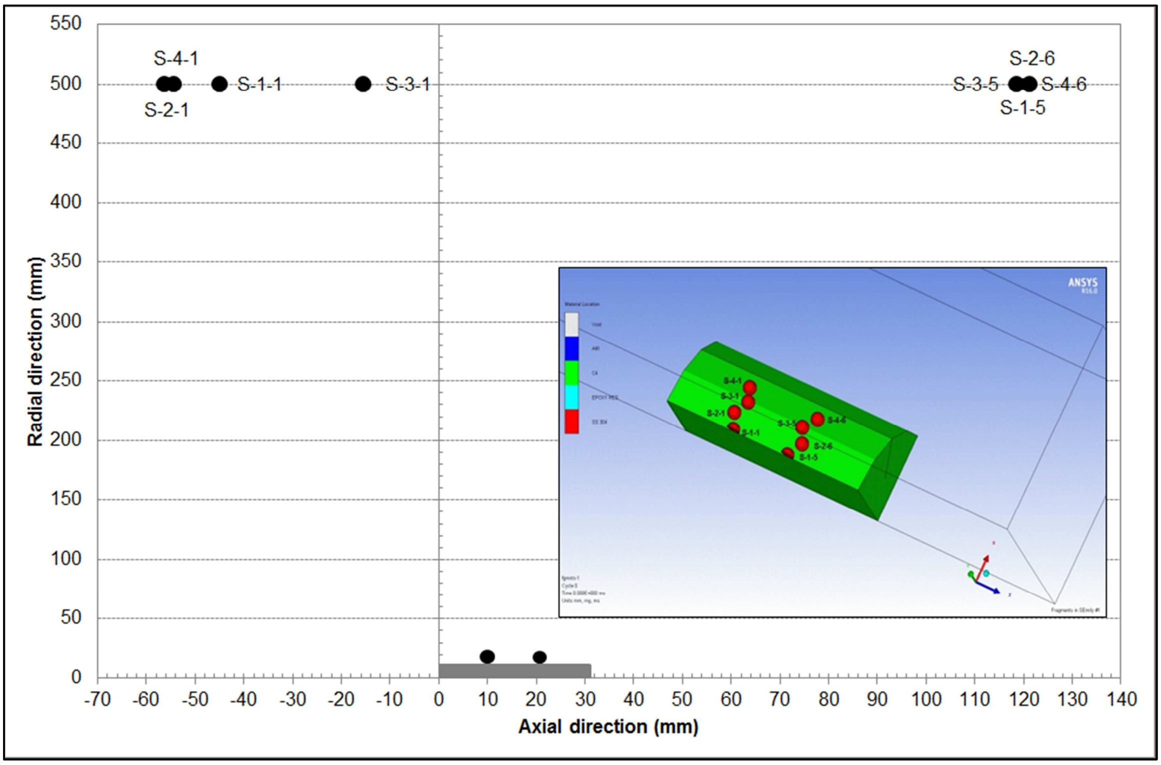

Figure 10: Extrapolation of positioning of spheres at 500 mm

Figure 11 shows the computed extreme positions of the spheres on the inside surface of SEmily adding an additional row towards the detonator side and the open side of SEmily. The spread was calculated to be 315 mm. Detonation is from left to right.

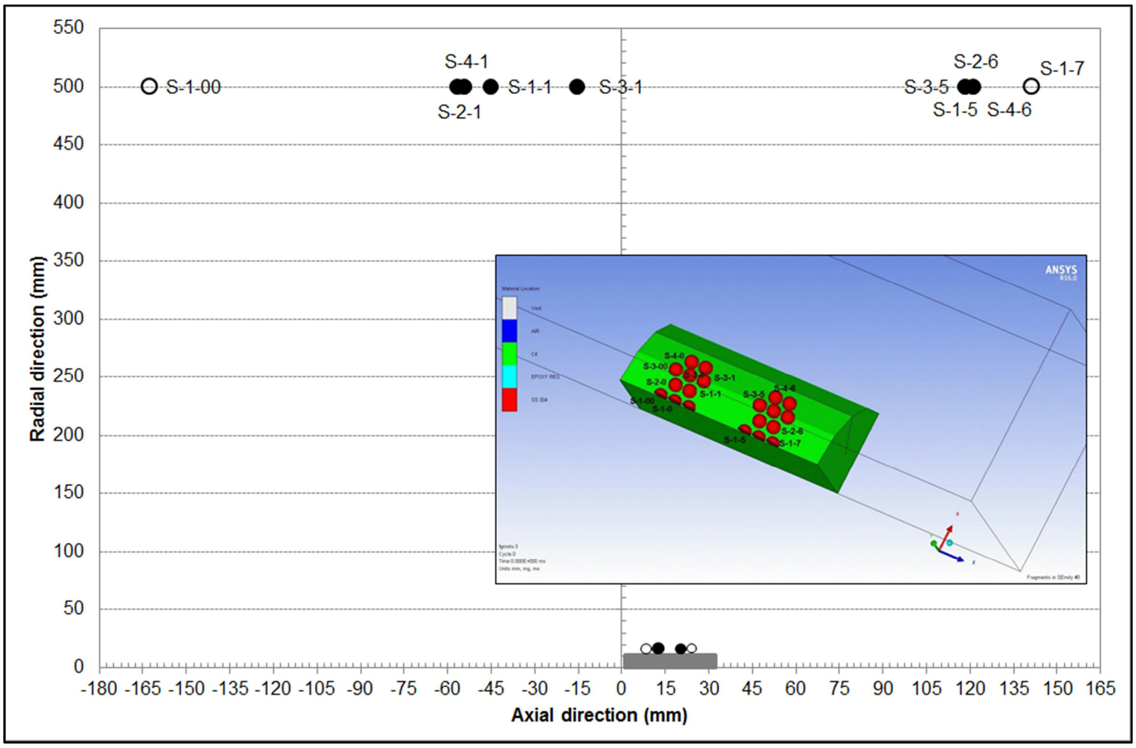

Figure 11: Extreme position of the spheres

Table 3 shows the computational results. Adding spheres to the side increases the spread. Adding one row towards the open end (in other words, away from the detonating side), does not affect the spread too much (by about 6%). However, adding an extra row towards the closed end of SEmily, that is, where the detonation point is, increases the spread considerably (almost 3 times).

Table 3: Spread of fragments at 500 mm from the axis of SEmily

Band width	Left most position	Right most position	Spread (mm)
10 mm	-54.2	129.5	196.8
SEmily open side 12 mm	-54.2	141.5	208.8
SEmily open and closed side 14 mm	-162.4	141.5	314.9

The bandwidth of 10 mm for the spherical balls (centre to centre) was used to construct the charge, as the calculated spread is adequate for SEmily.

5 EXPERIMENTAL RESULTS

The fragments were designed to achieve a terminal velocity of 1700 m/s. This parameter was not quantified during the test but was validated in the past two sets of experiments. The sacrificial materials were evaluated by counting the number of penetrations observed on the 3.2 mm buffer steel plate, measuring the depth of penetration and also inspecting the blast and thermal impacts on the surfaces of the sacrificial layer. The counting was done after each shot and the impact was marked. The shot was repeated with the same material and the number of penetrations in the buffer plate was counted.

5.1 Conveyor Belt

Figure 12 shows the Pareto type analysis of the number of penetration found on the buffer plate located behind the Conveyor belt sacrificial material after two shots. The majority of fragments had penetrated depth of 2 mm. The total number of penetrations on the buffer plate was 29 and the average spread of the fragments measured was found to be about 325 mm.

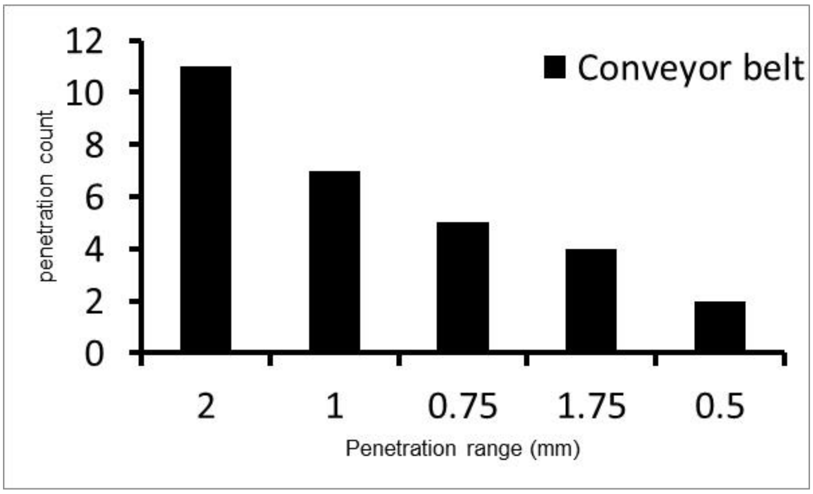

Figure 12: A Pareto representation of the penetration count against the depth range on the buffer steel plate.

The front part of the conveyor belt material is shown in Figure 13 and it seems to have withstood the heat and blast impact, as there appears to be no damage to the structural integrity even after two shots.

Figure 13: Exposed surface of conveyer belt material to fragments and blast, along the length of the chamber.

5.2 Supawood

Figure 14 illustrates the depth of penetrations on the backing buffer plate. The majority of fragments had penetrated depth of 1 mm. The number of penetrations on the buffer steel plate was found to be 18. The average spread of fragments on the buffer plate behind the material is 325 mm.

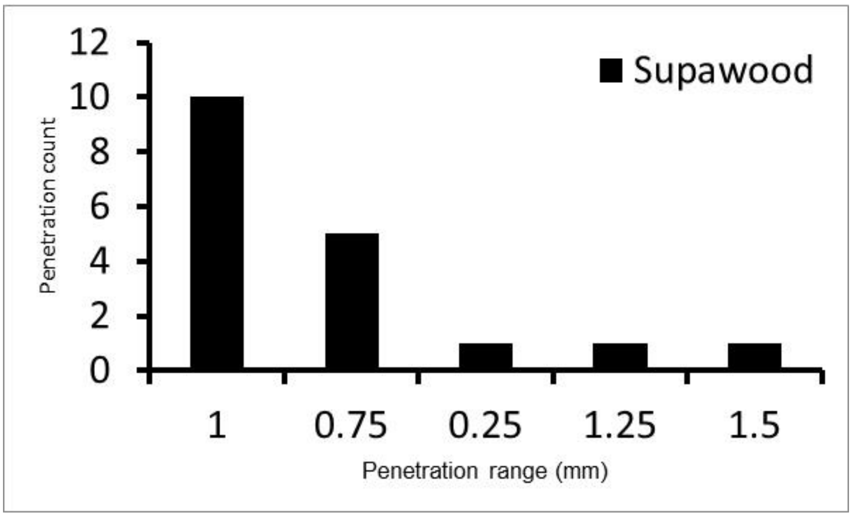

Figure 14: A Pareto showing the depth of penetration count on the buffer steel plate that backed the Supawood material.

Figure 15 shows the part of the front area of the Supawood material after the test. The structure of the material was still intact however; local discoloration was observed as shown which can be attributed to burning when this area was exposed to the blast and the fireball. The presence of the discoloration is concerning especially when enhanced devices with extended blast and thermal signature are characterised.

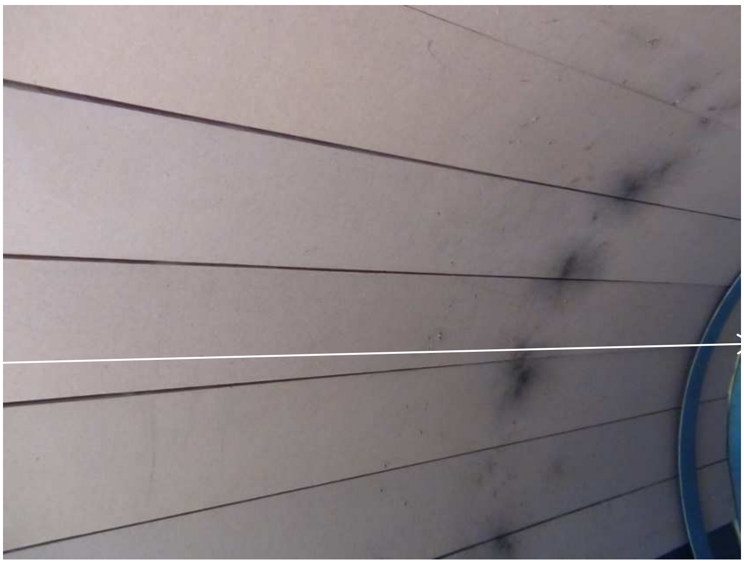

Figure 15: Exposed surface of Supawood material to fragments and blast, along the length of the chamber

5.3 Shutter Board

Figure 16 shows the depth of penetration on the steel buffer plate located behind the Shutter board material. The depth of penetration of the majority of the fragments penetrated was at 0.5 mm. The total number of penetrations on the buffer steel plate was 21. The average spread of fragments on the buffer plate behind the material is 420 mm which is a bit higher than predicted.

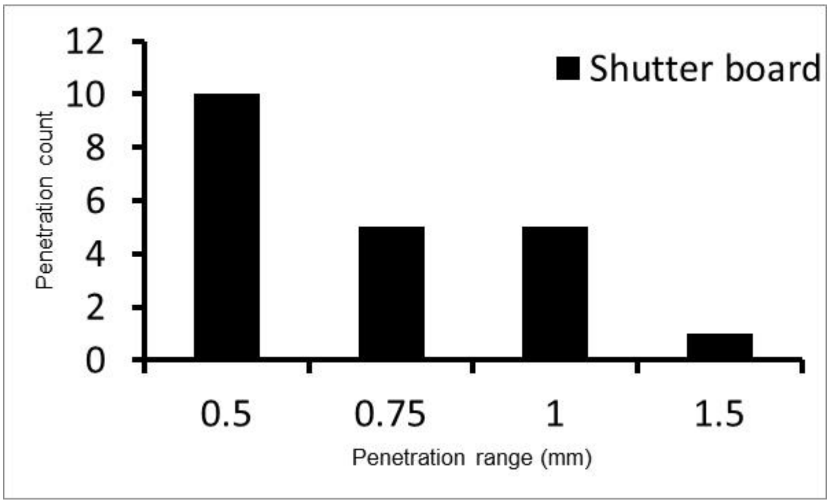

Figure 16: A Pareto illustrating the depth of penetration count on the backing buffer plate behind the Shutter board material.

Figure 17 shows the Shutter board material after the test. The shutter board material was still intact after the shot however, fewer discolorations were observed compared to that discussed on the Supawood.

Figure 17: Exposed surface of Shutter board material to fragments and blast, along the length of the chamber.

5.4 Polyurea/1.6 mm Steel Composite

For this composite material, no penetrations were observed on the 3.2 mm steel buffer plate which was located behind the material. There were no signs of damage or discolouration observed on the surface of the polyurea. The polyurea material was able to withstand the heat from the blast signature and fireball.

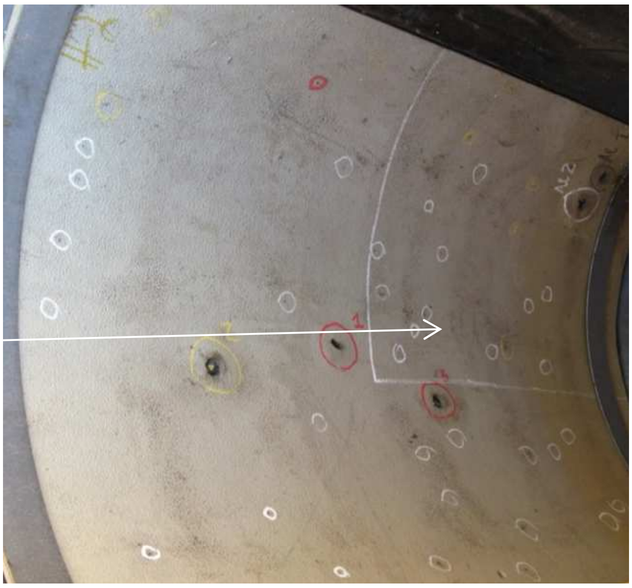

Figure 18: Exposed surface of Polyurea material to fragments and blast, along the length of the chamber.

6 DISCUSSION

Figure 19 shows the average and maximum penetration values on the 3.2 mm buffer steel plate. Polyurea/1.6 mm mild steel seems to offer the most protection. The error bars on the graph represent the standard deviations. The Shutter board follows the protection offered by the polyurea/1.6 mm mild steel. These two layers have shown that they can provide sacrificial protection in the confined blast environment to fragments. The conveyor belt and Supawood had the deepest penetration (2 mm) into the 3.2 mm buffer steel plate. These results are in agreement with the previous results from a fragment arena test.

Table 4 shows the average spread on the steel buffer plate and agree with the computational prediction.

Table 4: Average spread of the fragments on the steel buffer plate.

Material	Average spread (mm)
Conveyor belt	325
Supawood	325
Shutter board	420

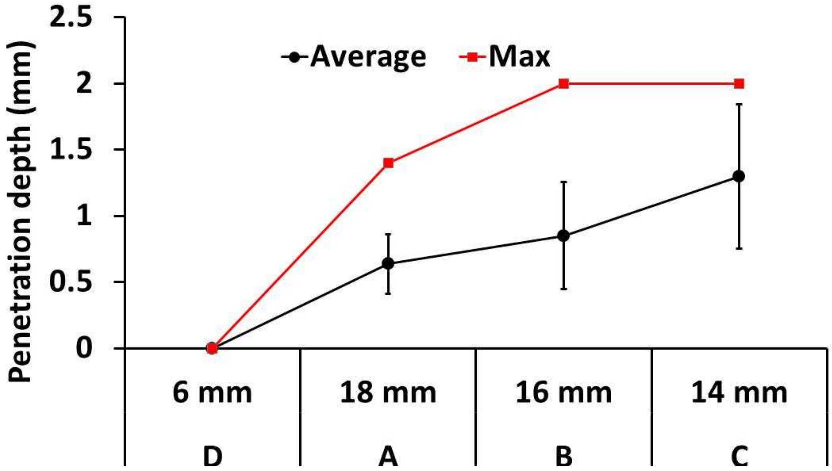

Figure 19: Average and maximum penetration depth on the buffer plate behind the evaluated sacrificial materials. The error bars represent the standard deviation.

7 CONCLUSION

The choice of sacrificial materials was based on the results of a previous study with an arena set-up that graded them according to their attenuation ability. The present study added the blast impact to the fragments in an enclosed environment.

The results on the penetration evaluation were in agreement with the previous test. The conveyor belt material performed the poorest of all the materials. It had the largest penetration count and the largest depths measured on the 3.2 mm buffer steel plate. The Polyurea/1.6 mm mild steel and shutter board layer offered the most protection as they resulted with the lowest penetration depth in the buffer plate. The Polyurea/1.6 mm composite captured all the steel balls and did not penetrate the buffer plate. The Shutter board material captured some of the steel balls while the others penetrated the buffer plate with low depths of penetration.

All the materials evaluated showed some degrees of resistance to the blast and thermal effects as their structural integrity was still undamaged and intact after the test. The Polyurea sheet was not affected by the thermal effects from the blast, as there was no discoloration observed on the material. The Shutter board almost suffered from thermal effects as there were fewer discolorations on the exposed area to the blast.

Based on these results, it is recommended that Polyurea/1.6 mm mild steel be used as the sacrificial layer for an enclosed blast chamber during the detonation of encased explosive charges, Emily. Shutter board can be used as well to substitute the Polyurea/1.6 mm mild steel, but to avoid the discolouration on the Shutter board and the probability of the material to catch fire, a thin steel plate can be used to cover the material. The recorded spread of the balls on the steel backing plate correlated with the range predicted from the mathematical models for the Conveyor belt and Supawood materials.

8 REFERENCES

KENNEDY, J.E., 1998. The gurney model of explosive output for driving metal. *Explosive Effects and Applications.* Springer, pp. 221-257.

SHOKE, L., SONO, T. and GRUNDLING, W., 2014. Evaluations of Sacrificial Materials for Lining the inside of a Blast Chamber , *Evaluations of Sacrificial Materials for Lining the inside of a Blast Chamber, South African Ballistics Organisation Conference. ,* 2014.

SNYMAN, I., MOSTERT, F. and OLIVIER, M., 2013. Measuring pressure in a confined space. *27th International Symposium On Ballistics, Freiburg, Germany,* .

SNYMAN, I., MOSTERT, F. and GRUNDLING, W., 2016. Design and commissioning of a semi-confined blast chamber. *Defence Technology,* 12(2), pp. 148-159.